

Brainstem raphe pallidus and the adjacent area contain a novel action site in the melanocortin circuitry regulating energy balance[☆]

Liugen Lei^{1,*}, Yan Gu², Jonathan G. Murphy², Pinxuan Yu⁴, James L. Smart⁴, Malcolm J. Low^{2,3,4}, Wei Fan²

¹Department of Human Anatomy, Basic Medical College, Zhengzhou University, Zhengzhou, Henan 450001, China; ²Center for the Study of Weight Regulation & Associated Disorders, ³Department of Behavioral Neuroscience, ⁴Vollum Institute, Oregon Health & Sciences University, Portland, OR 97239-3098, USA

Received December 23, 2007

Abstract

The central melanocortin system plays a critical role in the regulation of energy balance in rodents and humans. The melanocortin signals in both the hypothalamus and brainstem contribute to this regulation. However, how the melanocortin signals of the hypothalamus interact with those intrinsic to the brainstem in the regulation of energy balance is poorly understood. The brainstem raphe pallidus (RPa) and adjacent areas contain melanocortin 4 receptor (MC4-R)-bearing neurons and sympathetic premotor neurons regulating thermogenesis. Here we report that α -melanocyte-stimulating hormone (α -MSH)-immunoreactive (IR) fibers are in close apposition to MC4-R neurons in the RPa. Retrograde tracing studies revealed a unique direct projection from hypothalamic proopiomelanocortin (POMC) neurons to the RPa and adjacent areas of the brainstem in mice and rats. Furthermore, microinjection of the MC3/4-R agonist MTII into the RPa area dose-dependently stimulated oxygen consumption and inhibited feeding, whereas microinjection of the antagonist, SHU9119, enhanced feeding. These data suggest a novel pathway of hypothalamic POMC neuronal efferents to brainstem RPa area MC4-R neurons in the melanocortin circuitry that contribute to coordinate regulation of energy balance. [Life Science Journal. 2008; 5(3): 1 – 13] (ISSN: 1097 – 8135).

Keywords: melanocortin; food intake; thermogenesis; raphe pallidus; retrograde labeling; POMC

1 Introduction

The central melanocortin system plays a critical role in energy homeostasis in both rodents and humans^[1–4]. A simplified, bi-level model, including projections from the arcuate nucleus (Arc) to the hypothalamic nuclei, including the paraventricular nucleus of the hypothalamus (PVH), has been proposed for melanocortin regulation of energy balance^[5–9]. In this model, two sets of neurons, the proopiomelanocortin (POMC)- and agouti related protein (AgRP)-expressing neurons in the Arc/retrochiasmatic area (RCA) of the hypothalamus function as the first-order sites that integrate peripheral signals reflecting status of fuel storage and availability,

including anorectic signals such as leptin and insulin and the orexigenic signal ghrelin^[7,10–15]. Melanocortin 4 receptor (MC4-R) MC4-R-expressing neurons in the hypothalamus, including the PVH, function as the second-order or downstream integrative site to further process the homeostatic feedback signals thereby modulating output of MC4-R neurons to balance food intake and energy expenditure^[6,8,9]. However, it was recently argued that PVH MC4-R signaling may exclusively mediate appetite but not energy expenditure^[16].

In addition, the role of the brainstem nucleus of the solitary tract (NTS) POMC and MC4-R signaling in mediation of the satiety effect of cholecystokinin (CCK) has recently been revealed^[17,18]. Modulation of brainstem MC4-R activity by fourth ventricle or NTS injection of the MC3/4-R agonist MTII or antagonist SHU9119 alters food intake and meal size^[19–21], and fourth ventricle injection of MTII stimulates thermogenesis^[19,22,23]. Further-

*Supported by the National Institutes of Health DK62179 (WF) and DK 066004 (MJL).

[☆]Corresponding author. Email: leiliugen@hotmail.com

more, a small percentage of Arc POMC neurons directly project to the dorsal vagal complex (DVC)^[19]. These data highlight the importance of brainstem melanocortin integrative sites in the regulation of energy balance.

The sympathetic nervous system (SNS) plays a pivotal role in the regulation of energy expenditure^[24]. Within the brainstem RPa and its adjacent areas reside a subset of sympathetic premotor neurons that control thermogenesis and thermoregulation^[25–28]. The RPa area is a key relay site for the SNS, including melanocortin-mediated thermogenesis^[23,26,28–31]. Interestingly, MC4-R mRNA is expressed in the RPa and adjacent areas^[32–34]. However, both the source of melanocortin innervation and the potential functional roles of MC4-R neurons in the RPa area in the regulation of energy balance are unknown. Here, we sought to test the hypothesis that the RPa and the adjacent area may contain a novel action site in the melanocortin circuitry to coordinately regulate thermogenesis and food intake.

2 Materials and Methods

2.1 Animals and surgical procedures

All animals including Sprague-Dawley rats (male, 280 – 300 g for tracing studies, 280 – 400 g for feeding studies, Charles River Laboratories), C57BL/6J mice (male, 7 – 8 weeks old, Jackson Laboratories), MC4-R-GFP^[34] and NPY-GFP^[35] transgenic mice (provided by Dr. Jeffrey M. Friedman, The Rockefeller University), and POMC-EGFP transgenic mice^[10] were housed on a 12-h-light/dark cycle with food (Purina rodent Chow) and water available *ad libitum*. All experimental procedures were done in accordance with the NIH Guidelines on the Use and Care of Laboratory Animals and approved by the Animal Care and Use Committee of the Oregon Health & Science University.

The cannulations were performed generally as described before^[5]. Briefly, animals were anesthetized with a cocktail of ketamine/xylazine/acepromazine and placed in a stereotaxic apparatus (CARTESIAN Research, Inc., Sandy, OR). A sterile stainless steel guide cannula (25 G) with obturator stylet was stereotaxically implanted into the RPa (11.5 – 12.5 mm caudal to bregma, midline and 9.0 mm ventral to the skull surface for rat, according to the atlas of Paxinos and Watson, 1998; and 6.2 – 6.5 mm caudal to bregma, midline and 4.85 mm below the skull surface for mouse, according to the atlas of Paxinos and Franklin, 2001). The cannulae were then fixed in place with dental cement and screws. The animals were housed separately after surgery for at least 1 week for recovery

before experiments. The cannula position was verified at the end of experiments by histological analysis. In some rat experiments, cannula position was tested by dye injection prior to sacrifice. In most rat experiments, the tracks of guide cannulae were found between – 11.3 to – 11.8 mm posterior to bregma.

2.2 Retrograde tracing

Glass capillary pipettes (O.D. 1.00 mm) with a 15 – 30 μm tip for mice, or a 25 – 50 μm tip for rats were filled with 0.5% cholera toxin B (CTB, List Biological Laboratories, Campbell, CA) in sterile saline. 100 – 200 nl of CTB was stereotaxically injected into the mouse RPa (6.2 – 6.5 mm caudal to bregma, midline, 5.9 mm below the skull surface); for anatomic control injections, 40 – 50 nl of CTB was injected stereotaxically into the Gi (5.95 – 6.15 mm caudal to bregma, L: 0.35 – 0.4 mm, H: 5.12 – 5.25 mm), and 100 – 200 nl of CTB into the rat RPa (12.5 mm caudal to bregma, midline, 10.5 mm below the skull surface) with aid of the Pressure System IIe (Toohey Company) or nanoject II (Drummond Scientific Company). At the end of the pressure injection, pipettes were left in place for an additional 10 minutes to minimize tracer leakage along the pipette tract. The mice or rats were allowed survival for 4 – 5 days and 7 days, respectively, for retrograde transport.

2.3 Immunocytochemistry

The animals were deeply anesthetized and transcardially perfused with PBS followed by chilled 4% paraformaldehyde in 0.1 M PBS (pH 7.4). The brains were postfixed, cryoprotected with 20% sucrose and cut into 30 μm coronal sections on a cryostat (Leica CM1900). For detection of α -MSH-IR fibers and MC4-R-GFP-IR neurons, 2% paraformaldehyde and 4% acrolein in 0.1 M PBS (pH 7.4) were used, and serial 25 μm sections through the RPa were cut using a vibratome. The sections were treated for 30 minutes with 1% sodium borohydride, followed by 0.5% H₂O₂ in PBS for 15 minutes. For mapping of α -MSH-IR fibers, sections were incubated with 5% normal donkey serum in PBS then with sheep anti- α -MSH polyclonal antibody (1 : 40000; Chemicon International, Temecula, CA) for 48 hours at 4 °C. Sections were rinsed in PBS and subsequently incubated with biotin-SP-conjugated donkey anti-sheep IgG (1 : 400; Jackson ImmunoResearch Laboratories, Inc) for 3 hours at room temperature (RT). The sections were incubated in the avidin-biotinylated peroxidase complex (Elite ABC kit; 1 : 100; Vector Laboratories, Burlingame, CA) in 0.01 M PBS for 2 hours at RT followed by biotinyl tyramide amplification reagent (1 : 50; New England Nuclear, Bos-

ton, MA) for 10 minutes at RT. The sections were further incubated for 2 hours with streptavidin, Alexa Fluor 594 conjugated (1 : 1000; Molecular Probes, Inc). For immunofluorescent labeling MC4R-GFP, rabbit anti-GFP IgG conjugated with Alexa Fluor 488 (1 : 500, Molecular Probes, Inc) was used. Detection of AgRP-IR fibers in the RPa followed the same procedures as α -MSH-IR staining. Rabbit anti-AgRP polyclonal antibody (1 : 15000; Phoenix Pharmaceuticals, Mountain View, CA) was used. The immunoreaction product was developed by using DAB/nickel chromogen.

For double labeling of CTB and POMC-GFP or NPY-GFP, sections from mouse brain were incubated in goat antiserum to CTB-subunit (anti-cholera toxin, 1 : 20000, List) in blocking solution for 48 hours at 4 °C followed by biotinylated horse anti-goat IgG (Vector Laboratories, Inc.) and streptavidin conjugated Alexa Fluor 594 (Molecular Probes, Inc.). Sections were further incubated in rabbit anti-GFP IgG conjugated Alexa Fluor 488 (Molecular Probes, Inc.) overnight at 1 : 500 dilution.

For double labeling of CTB and POMC in the rat, sections were incubated simultaneously with rabbit anti-porcine POMC precursor^[27–52] serum (Phoenix Pharmaceuticals, Inc) at 1 : 3000 and goat antiserum to cholera toxin B-subunit (anti-cholera toxin, 1 : 20000, List) followed by biotin-SP-conjugated donkey anti-rabbit IgG (Jackson ImmunoResearch Laboratories, Inc) and streptavidin conjugated Alexa Fluor 488 (Molecular Probes, Inc). Thereafter, Cy3-conjugated donkey anti-goat IgG (Jackson ImmunoResearch Laboratories, Inc) was used to visualize the CTB immunoreaction product. Sections were mounted and coverslipped with Gel/Mount (Biomedica Corp.).

POMC and CTB-IR neurons were quantitatively analyzed for co-localization based on four mice with CTB injection sites confined to the RPa and adjacent area. Hypothalamic POMC neurons were included in three divisions: RCA, rArc, and cArc, corresponding to the sections of – 1.06 mm, – 1.46 mm and – 1.82 mm posterior to bregma, respectively (Paxinos and Franklin, 2001). Three 30 μ m coronal sections from the adjacent planes of each division were chosen. POMC and CTB-IR neurons in both sides of the Arc were counted under the 10 \times objective of a Zeiss Axioplan 2 microscope. Double-labeled neurons were determined under a Zeiss fluorescent microscope by switching between red and green filters.

2.4 Feeding assay

On the test days, food was removed 2 hours prior to lights off (1800). A single dose of MTII (0.03 nmol and 0.3 nmol, 0.3 μ l; or 0.03 nmol and 0.1 nmol, 0.1 μ l) or SHU9119 (0.1 nmol, 0.3 μ l; or 0.03 nmol and 0.1 nmol,

0.1 μ l) or ACSF (0.3 μ l and 0.1 μ l) were administered with a 32 G injection tube protruding 1.5 mm out of a guide cannula over a period of 2 – 3 minutes with a micrometer head (The LS starrett) 1 hour before start of the dark phase. Pre-weighed rodent chow was presented in the cage following the RPa microinjection and food intake was measured at the time intervals indicated. Control and treated animals were switched after a 5 – 7 days recovery and the experiment was repeated.

2.5 Indirect oxygen consumption measurement

Mice were allowed to adapt to the experimental conditions by being placed in the chambers of an indirect open-circuit calorimeter (Oxymax, Columbus Instruments) for the experimental time period each day for 2 days. On the day of experiment, after about a 2-hour (10:00 – 12:00 A.M.) acclimatization, the mice were briefly removed from the calorimeter for RPa microinjection of either MTII (0.5 nmol, 0.2 μ l; or 0.1 and 0.5 nmol, 0.1 μ l) or ACSF (0.2 μ l and 0.1 μ l) over a period of 2 – 3 minutes with the injection tube protruding 1 mm out of the guide cannula. The animals were then put back in the measurement chambers. Oxygen consumption was recorded for 3 hours with an inlet fresh air flow rate of 0.6 L/min and a sample flow rate of 0.5 L/min.

The doses used for RPa injection during mouse oxygen consumption experiments and during rat food intake experiments were based on published literature^[5,19–21] and our preliminary experiments.

2.6 Data analysis

All data were presented as mean \pm SEM. For feeding assays, significance of drug effects was determined by two-way ANOVA. For oxygen consumption assays, an unpaired, two-tailed *t*-test was used for comparison between groups. *P* < 0.05 was considered statistically significant.

3 Results

3.1 Distribution of melanocortins in the brainstem RPa area

With the aid of tyramide signal amplification (TSA), α -MSH-immunoreactive (IR) fibers were observed in the RPa and NTS of brainstem in mice (Figure 1 A, C, E, G, H). The α -MSH-IR fibers were also seen sparsely distributed in adjacent regions including the raphe magnus nucleus (RMg) and raphe obscurus nucleus (ROb) (data not shown). The distribution of α -MSH-IR fibers in the RPa of the rat exhibited a similar pattern as in mice (data not shown). Dense AgRP-IR fibers were readily seen

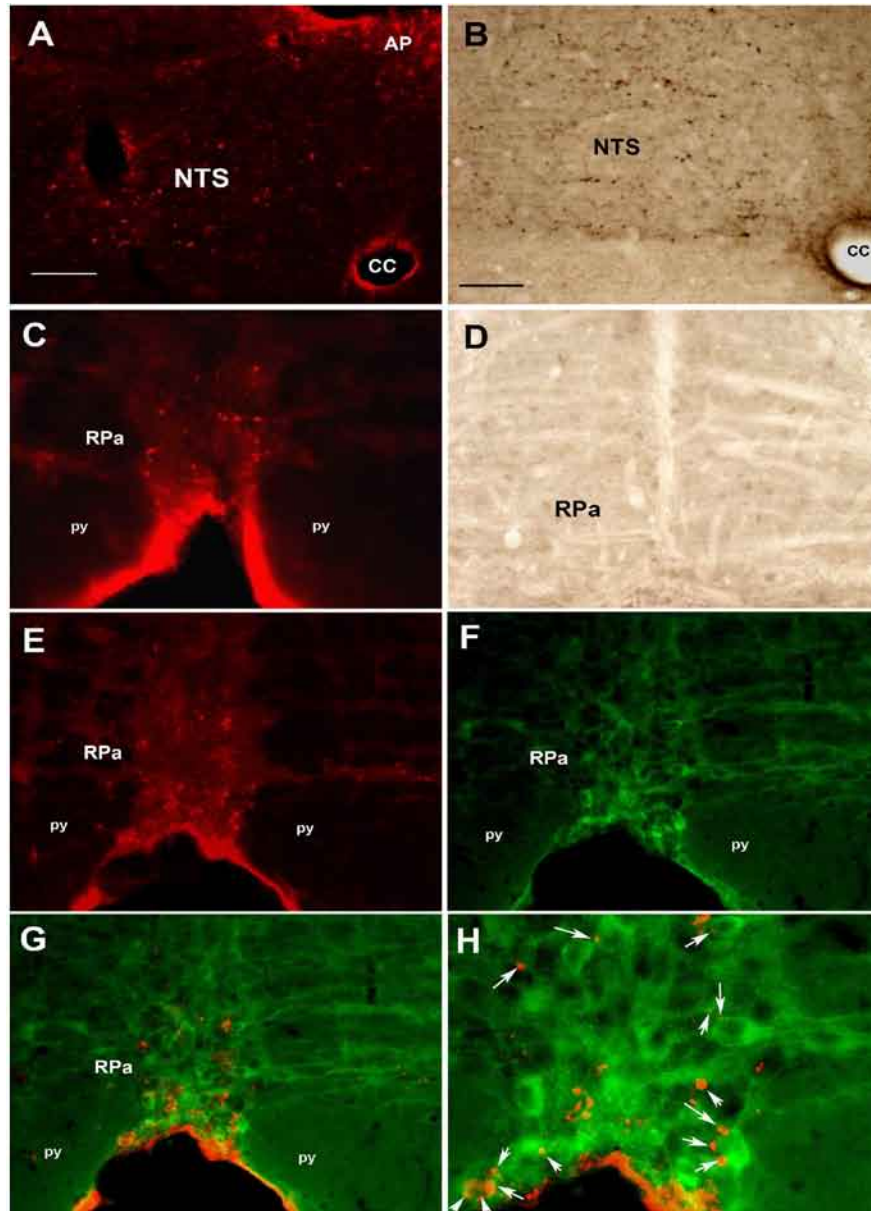


Figure 1. Photomicrograph showing the distribution of melanocortin peptides in the brainstem of the mouse brain. (A): α -MSH-IR fibers in the NTS. (B): AgRP-IR fibers in the NTS. (C): α -MSH-IR fibers in the RPa area. (D): Absence of AgRP-IR in the RPa area. (E – F): Dual-label fluorescence ICC demonstrated that α -MSH-IR axons (red, E, G) were in close apposition to the MC4-R-GFP-IR neurons (green, F, G) in the RPa. G is merged image of D and E. (H): is a high magnification image of α -MSH-IR varicosities (red; white arrow) contacting the cell body of MC4-R-GFP-IR neurons (green). Abbreviations: py, pyramidal tract; cc, central canal, RPa, raphe pallidus, NTS, the nucleus of solitary tract. Scale bar: 50 μ m for A – F.

in the NTS (Figure 1 B), whereas few AgRP-IR fibers were detected in the RPa and adjacent areas (RMg and ROb) in mice (Figure 1, D). Next, we used MC4-R-GFP transgenic mice to characterize the distribution of melanocortin-target neurons in the RPa area. These mice have been reported to exhibit an identical CNS distribution of GFP-positive cells to that of MC4-R mRNA positive cells

and nearly all GFP-producing cells co-express MC4-R mRNA^[34]. MC4-R-GFP-IR neurons were seen throughout the RPa, RMg and ROb, and they formed columns along the ventro-dorsal plane (Figure 1 F – H). Using standard dual fluorescence immunocytochemistry (ICC), we found that α -MSH-IR varicosities were in close apposition to MC4-R-GFP-IR neurons in the RPa (Figure 1 G – H).

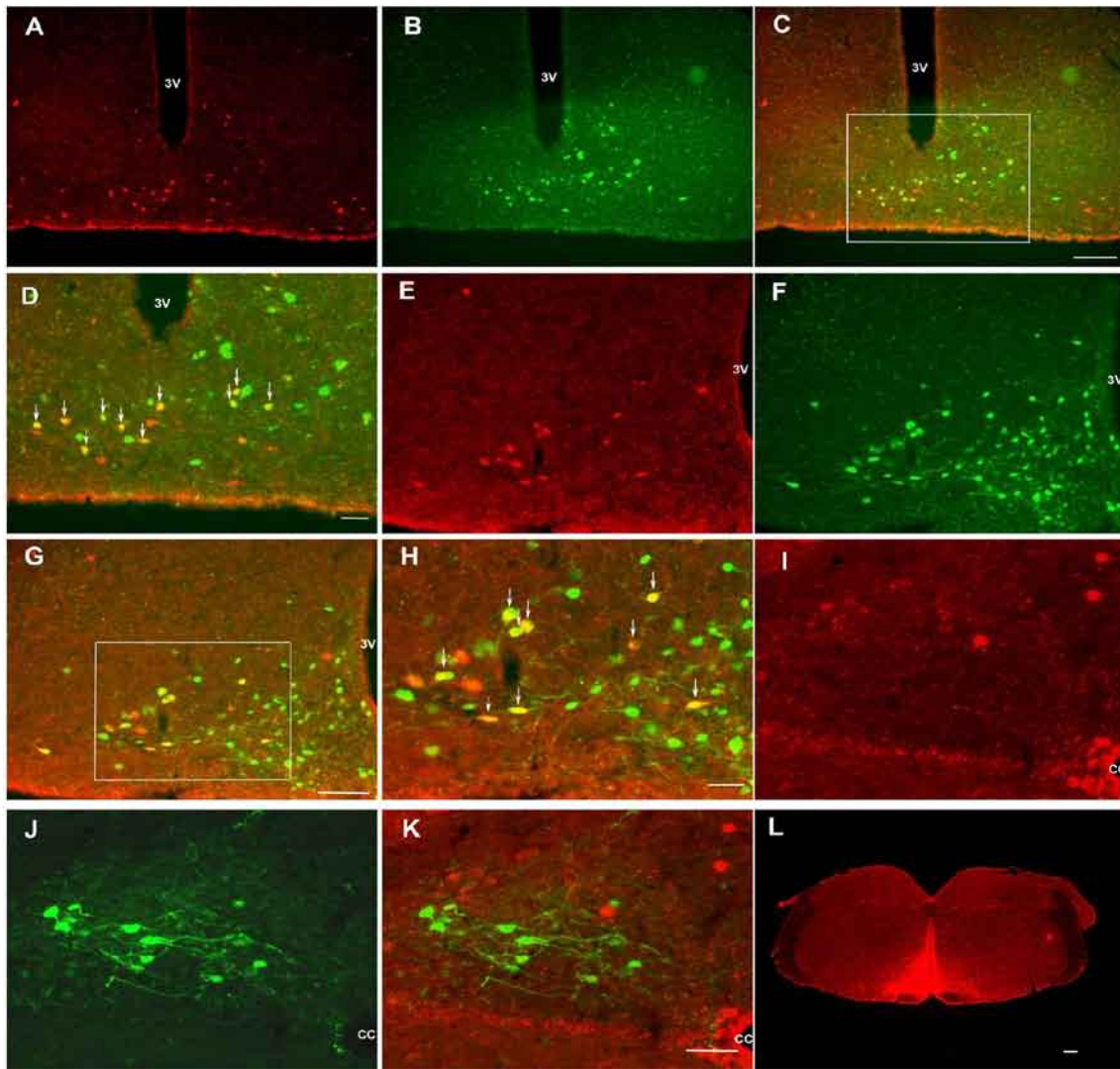


Figure 2. Hypothalamic POMC neurons project to the RPa and the adjacent area in POMC-EGFP transgenic mice. (A – C): Distributions of CTB-IR (red, A), POMC-EGFP (green, B), and double-labeled neurons in the RCA (yellow, C, merged image of A and B). (D): Higher magnification of boxed area in C showing double-labeled neurons of CTB-IR and POMC-EGFP (yellow, arrows). (E – G): Distribution of CTB-IR (red, E), POMC-EGFP (green, F), and double-labeled (yellow, G, merged image of E and F) neurons in the Arc. (H): Higher magnification of boxed area in G showing double-labeled neurons of CTB-IR and POMC-EGFP (yellow, arrows). (I – J): Distribution of CTB-IR (red, I) and POMC-EGFP-IR (green, J) neurons in the NTS. (K): Merged image of I and J shows that no double labeling of CTB-IR and POMC-EGFP-IR neurons could be found in the NTS. (L): A representation of the injection site of CTB in the RPa and adjacent area. Abbreviations: 3v, third ventricle. Scale bar: 100 μ m (A – C and E – G); 50 μ m (D, H and I – K); 200 μ m (L).

These data suggest that MC4-R neurons in the RPa area may receive synaptic innervation from POMC neurons, but not from AgRP neurons.

3.2 Origin of the α -MSH-IR fibers in the RPa area

To further investigate the origin of the α -MSH-IR fibers in the RPa area, we conducted retrograde tracing coupled with dual ICC using POMC-EGFP transgenic mice, in which the specificity of hypothalamic EGFP expression to POMC neurons has been confirmed^[10]. The retrograde

tracer cholera toxin subunit b (CTB) was injected into the RPa region. In four cases of RPa CTB injection, many CTB-IR neurons were found in the hypothalamic RCA (Figure 2 A) and the lateral portion of the Arc (Figure 2 E). However, only a few CTB-IR neurons were found in the cNTS of brainstem (Figure 2 I). Neurons expressing POMC-EGFP were observed in the RCA/Arc of the hypothalamus (Figure 2 B, F) and the cNTS of brainstem (Figure 2 J). POMC-EGFP neurons in the RCA (Figure 2 C, D), rArc (Figure 2 G, H) and cArc were found to

Table 1. Quantitative estimate of mouse brain POMC neurons projecting to the RPa and adjacent area

Region	CTB-IR neurons	POMC-EGFP neurons	Double-labeled neurons (CTB+POMC)	% Double-labeled of POMC neurons	% Double-labeled of CTB-R neurons
RCA	19.8 ± 2.7	32.3 ± 4.7	11.9 ± 1.9	37.1 ± 3.2	60.3 ± 6.8
rArc	34.1 ± 3.0	166.1 ± 16.9	13.1 ± 1.6	8.1 ± 1.3	38.1 ± 2.6
cArc	8.5 ± 1.4	101.2 ± 11.5	4.0 ± 0.6	3.9 ± 0.7	50.2 ± 5.8
Arc-average	20.8 ± 2.4	99.9 ± 11.0	9.7 ± 1.4	16.4 ± 1.7	49.4 ± 5.1
cNTS	16.0 ± 3.1	32.3 ± 5.9	– 0	– 0	– 0

Values represent mean ± SEM ($n = 4$). Three divisions of the hypothalamus: RCA, rArc, cArc and cNTS in the medulla correspond to the sections of – 1.06 mm, – 1.46 mm, – 1.82 mm and – 7.48 mm posterior to bregma, respectively, according to the atlas of Paxinos and Franklin (2001). Abbreviation: RCA, retrochiasmatic area of the hypothalamus; rArc, rostral arcuate nucleus of the hypothalamus; cArc, caudal arcuate nucleus of the hypothalamus; cNTS, caudal half of the commissural nucleus of the tractus solitarius.

contain CTB-IR (Table 1). The injection sites covered the RPa, RMg, ventral parts of ROb and the gigantocellular reticular nucleus, α part (GiA) (Figure 2 L). Quantification of the hypothalamic POMC-EGFP neurons projecting to the RPa region revealed an average of 16 % of the hypothalamic POMC-EGFP neurons contained CTB-IR, and an average of 49 % of CTB-IR neurons in the Arc/RCA were POMC-EGFP positive (Table 1). No co-expression of CTB-IR and POMC-EGFP-IR was found in the cNTS (Figure 2 K, Table 1).

To further confirm the above results, we repeated the CTB retrograde tracing study in rats. In three cases the injection sites covered the RPa (Figure 3 L). A specific subset of POMC-IR neurons in the Arc/RCA of the hypothalamus were found to contain the CTB-IR whereas no POMC-IR neurons in the cNTS contained CTB-IR (Figure 3 A – K).

For anatomic controls, we examined injections of the retrograde tracer into areas adjacent to the RPa of POMC-EGFP transgenic mice. In one case, the injection site of CTB was lateral to the RPa in one side of GiA and RMg. CTB-IR neurons were still found in the hypothalamic RCA, and some of them co-expressed POMC-EGFP. A few CTB-IR neurons were seen in the lateral portion of the Arc and the cNTS of the brainstem. Co-expression of CTB-IR and POMC-EGFP-IR was not found in the cNTS. In 3 other cases, the injection sites were in various parts of the gigantocellular reticular nucleus (Gi), which were more dorsal and lateral to the GiA and did not include the RPa or RMg. In one case, 2 CTB-IR cells were found co-expressed with POMC EGFP in both the RCA and Arc, respectively, whereas one CTB-IR cell co-expressed POMC EGFP-IR in the cNTS. In another case, one CTB-IR neuron co-expressed POMC EGFP in several RCA/Arc sections. In the third case, 4 CTB-IR cells co-expressed POMC EGFP in the RCA (data not shown).

We next conducted a retrograde tracing study using

NPY-GFP transgenic mice. It was previously shown that almost all Arc NPY neurons co-express AgRP^[35–37]; thus, the Arc NPY-GFP neurons were used as an alternative marker for Arc AgRP neurons^[35]. In two cases of CTB injections into the RPa and adjacent regions, the distribution of CTB-IR and NPY-GFP-IR neurons were found in different patterns in the Arc. CTB labeled neurons resided both more laterally and mediodorsally (supplementary Figure 1 A), while NPY-GFP-IR neurons resided approximately medioventrally (supplementary Figure 1 B). Few examples of co-expression of CTB-IR and NPY-GFP-IR were observed in this study (supplementary Figure 1 B C, D).

Taken together, these data suggest that the MC4-R-expressing neurons in the RPa and adjacent area may receive innervations from hypothalamic POMC neurons, but not from POMC neurons of the NTS nor from hypothalamic AgRP neurons.

3.3 Activation of MC4-R in the RPa area stimulates oxygen consumption

The RPa and adjacent area contain the putative sympathetic premotor neurons that regulate thermogenesis. MC4-R-expressing neurons reside in the RPa area, and MC4-R-expressing neurons in the RPa polysynaptically contact interscapular brown adipose tissue (IBAT)^[38]. We thus tested the hypothesis that the RPa and adjacent area may be one of the putative action sites for melanocortin-regulated thermogenesis. Microinjection of MC3/4 agonist MTII into the RPa area (0.5 nmol, 0.2 μ l) significantly increased oxygen consumption compared with vehicle control in C57BL/6J mice (Figure 4 A, $n = 7$, $P < 0.001$). In two contrasting cases, MTII (0.5 nmol, 0.2 μ l, microinjected into the Gi or dorsal ROb, which did not include GiA, RMg and RPa, did not stimulate oxygen consumption in mice compared with the vehicle (data not shown). Furthermore, in a separate experiment using

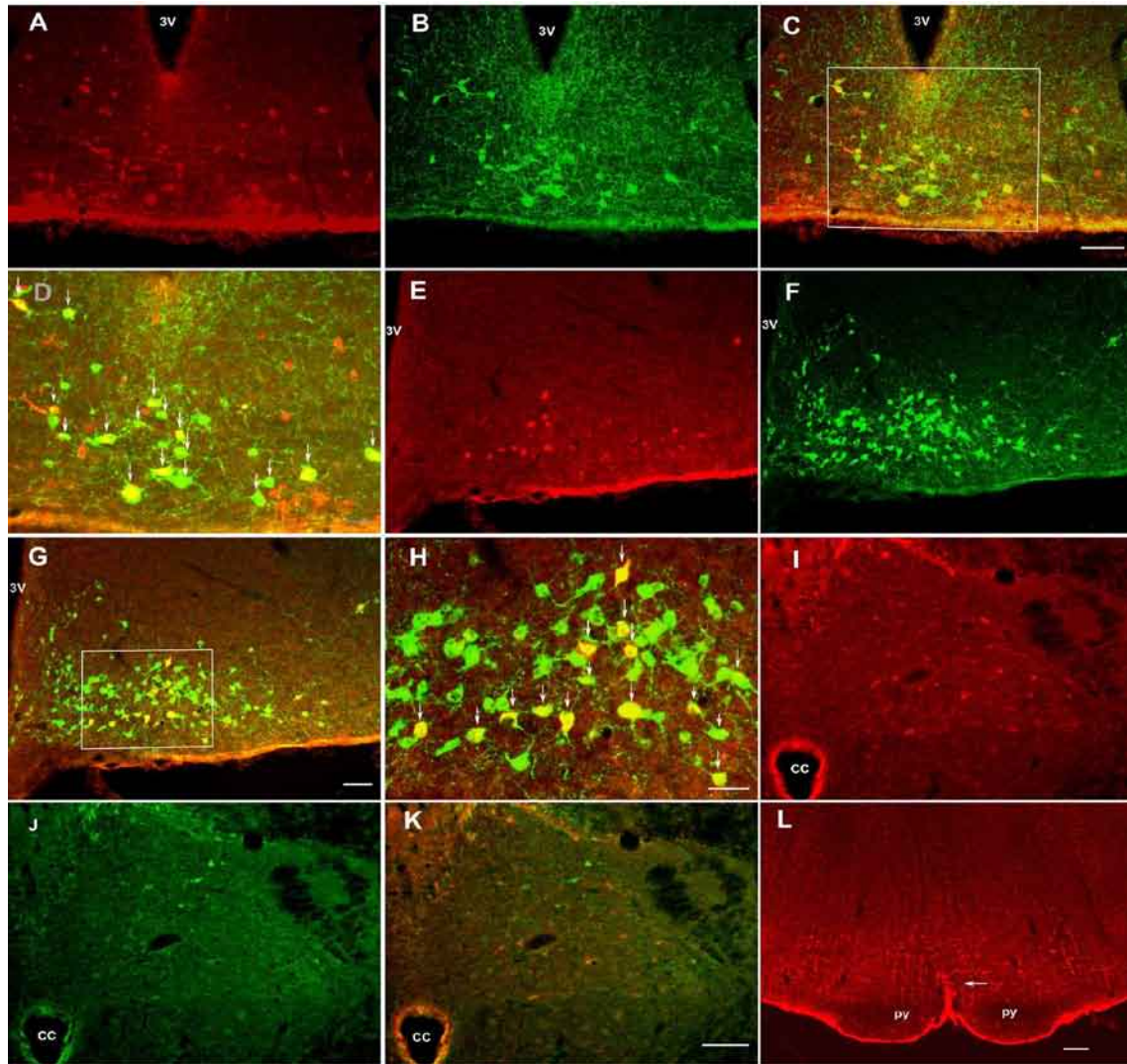


Figure 3. Hypothalamic POMC neurons project to the RPa and adjacent area in the rat. (A – C): Distributions of CTB-IR (red, A), POMC-IR (green, B), and double-labeled (yellow, C, merged image of A and B) neurons in the RCA. (D): Higher magnification of boxed area in C shows double-labeling of CTB-IR and POMC-IR neurons (yellow, arrows). (E – G): Distribution of CTB-IR (red, E), POMC-IR (green, F), and double-labeled (yellow, G, merged image of E and F) neurons in the Arc. (H): Higher magnification of boxed area in G shows double-labeling of CTB-IR and POMC-IR (yellow, arrows) neurons. (I – J): Distribution of CTB-IR (red, I), POMC-EGFP-IR (green, J) neurons in the NTS. (K): Merged image of I and J showing that no double labeled neurons of CTB-IR and POMC-EGFP-IR could be found in the NTS. (L) The injection site of CTB in the RPa area (white arrow). Scale bar: 100 μ m (A – C, E – G, I – K); 50 μ m (D, H); 200 μ m (L). Abbreviation: 3v, third ventricle; py, pyramidal tract.

reduced doses and injection volume, we found that micro-injection of MT II (0.1 or 0.5 nmol, 0.1 μ l) into the RPa area dose-dependently stimulated oxygen consumption in C57BL/6J mice (Figure 4 D). The average oxygen consumption over three hours was (3014.0 \pm 121. 3) ml/kg/h for the ACSF group (n = 5); (3488.0 \pm 82.1) ml/kg/h for MTII 0.1 nmol, 0.1 μ l group (n = 3), P < 0.05, and (4190.0 \pm 123.0) ml/kg/h for MTII 0.5 nmol, 0.1 μ l group (n = 3), P < 0.001 (Figure 4 D). The localization of injection sites was histologically confirmed at the end of experiments

(Figure 5 A).

3.4 Melanocortin release in the RPa area inhibits food intake

As food intake is coordinately regulated with energy expenditure by MC4-R signaling, we next tested the hypothesis that MC4-R signaling in the RPa area may also regulate food intake. RPa microinjection of MTII (0.03 nmol and 0.3 nmol, 0.3 μ l) significantly decreased nocturnal food intake in rats in a dose-dependent manner (Fig-

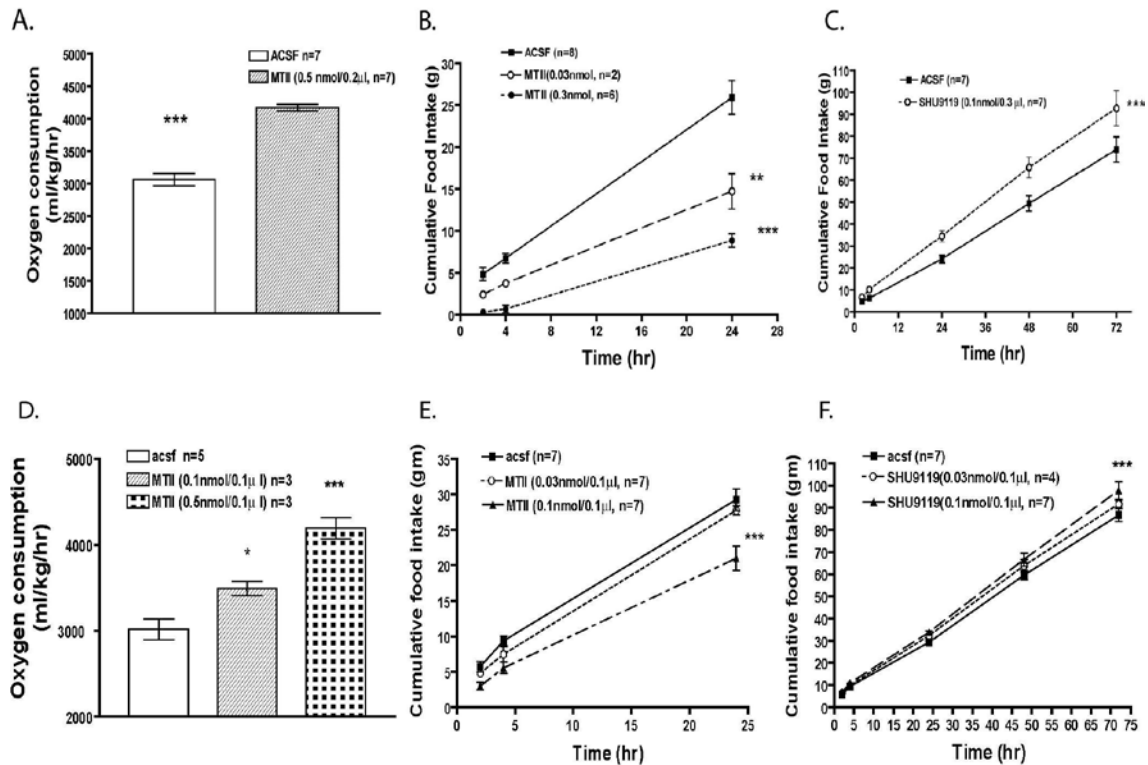


Figure 4. Effects of the RPa melanocortins on oxygen consumption and food intake. (A): Microinjection of MTII (0.5 nmol, 0.2 μ l) into the RPa area significantly increases oxygen consumption in C57BL/6J mice ($n = 7$, $P < 0.001$). (B): Microinjection of MTII (0.03, 0.3 nmol, 0.3 μ l) into the RPa area of rats significantly inhibits food intake in a dose dependent manner ($P < 0.001$). (C): Microinjection of SHU9119 (0.1 nmol, 0.3 μ l) into the RPa area significantly increases food intake in rats ($n = 7$, $P < 0.001$). (D): Microinjection of MTII (0.1, or 0.5 nmol, 0.1 μ l) into the RPa area significantly increases oxygen consumption in C57BL/6J mice. (*: $P < 0.5$; ***: $P < 0.001$). (E): Microinjection of MTII (0.03, or 0.1 nmol, 0.1 μ l) into the RPa area of rats significantly inhibits food intake in a dose dependent manner (***: $P < 0.001$). (F): Microinjection of SHU9119 (0.03 or 0.1 nmol, 0.1 μ l) into the RPa area of rats increases food intake in a dose dependent manner (***: $P < 0.001$).

ure 4 B, $P < 0.001$). In contrast, RPa administration of the MC3/4-R antagonist SHU9119 (0.1 nmol, 0.3 μ l) significantly increased cumulative food intake in rats (Figure 4 C, $P < 0.001$). Moreover, in a separate experiment using reduced doses and injection volume, we found that microinjection of MTII (0.03 and 0.1 nmol, 0.1 μ l) still dose-dependently decreased nocturnal food intake, whereas SHU9119 (0.03 and 0.1 nmol, 0.1 μ l) dose-dependently stimulated food intake in a separate experiment (Figure 4 E, F). However, when SHU9119 (0.3 nmol, 0.3 μ l, $n = 2$) was microinjected into the Gi, or dorsal ROb, which are more dorsal or lateral to, but do not include GiA, RMg and RPa, no stimulatory feeding effect of SHU9119 was observed. Microinjection of MTII (0.3 nmol, 0.3 μ l, $n = 2$) into the parvicellular reticular nucleus (PCrT) and intermediate reticular nucleus (IRt) did not inhibit food intake (data not shown). The placement of injection sites was histologically verified at the end of experiments (Figure 5

B). Interestingly, a stimulatory effect on food intake was also observed following administration of SHU9119 (0.3 nmol, 0.3 μ l) into the Gi A ($n = 4$, $P < 0.01$, supplementary Figure 2). These data suggest that MC4-R signals in the RPa and adjacent area may exert a tonic inhibition on food intake.

4 Discussion

Melanocortin signals in both the hypothalamus and brainstem play a pivotal role in energy homeostasis^[7,17,19-23,39,40]. While a small percentage of Arc POMC neurons directly project to the DVC^[19], the results presented here reveal that the neurons in the brainstem RPa region receive a novel direct projection from a subset of hypothalamic POMC neurons. The melanocortin agonist α -MSH-IR terminal fibers are distributed in the RPa in proximity to MC4-R-GFP-IR neurons. We also demonstrate that

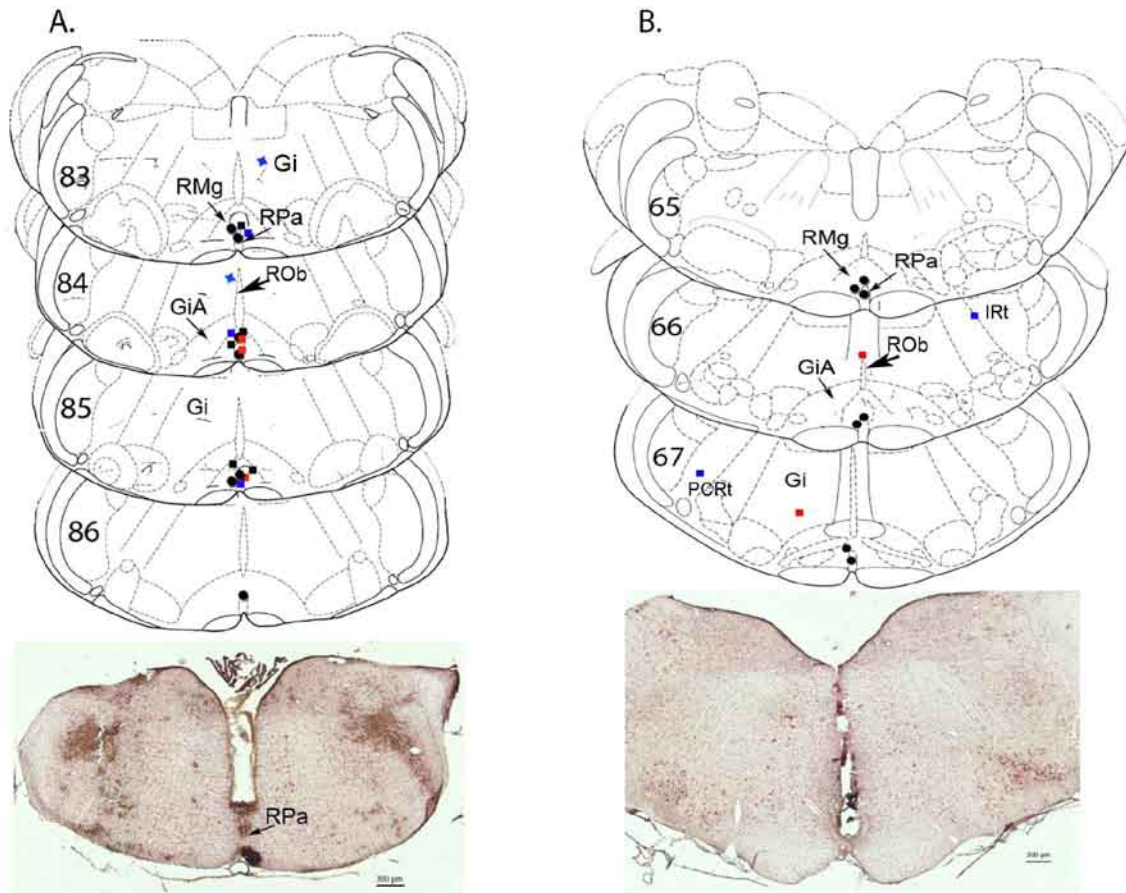


Figure 5. Localization of the RPa microinjection sites in mice (A) and rat (B). (A): The placement of microinjection sites with guide cannulae aimed at the RPa of mice are shown on modified atlas drawings approximately from 6.24 to 6.64 mm caudal to bregma, with the atlas figure numbers on the left side of each section (Paxinos, 2001). Filled black circles indicate the locations of dye spots marking the injection sites in the RPa region of the ventromedial medulla in 7 mice (ACSF/MTII 0.5 nmol, 0.2 μ l). The black squares indicate the RPa 0.1 μ l ACSF injection sites; the blue squares indicates the RPa MTII (0.1 nmol, 0.1 μ l) injection sites and the red squares indicate the RPa MTII (0.5 nmol, 0.1 μ l) injection sites. The blue stars indicate the Gi/ROb MTII (0.5 nmol, 0.2 μ l) control injection sites. A photomicrograph of a representative histological coronal section containing a microinjection site in the RPa region of the ventromedial medulla of mouse is shown on the bottom. Scale bar: 300 μ m. (B): The placement of microinjection sites with guide cannulae aimed at the RPa of rat are shown on modified atlas drawings approximately from 11.3 to 11.8 mm caudal to bregma, with the atlas figure numbers on the left side of each section (Paxinos, 1998). Filled circles indicate the locations of dye spots marking the injection sites in the RPa region of the ventromedial medulla in 7 rats for MTII/SHU9119 (0.3 nmol, 0.3 μ l). Red squares indicate the Gi/ROb SHU9119 (0.3 nmol, 0.3 μ l) control injection sites, and blue squares indicate the parvicellular reticular nucleus (PCrT) and intermediate reticular nucleus (IRt) MTII (0.3 nmol, 0.3 μ l) injection sites. A photomicrograph of a representative histological coronal section containing a microinjection site in the RPa region of the ventromedial medulla of rat is shown on the bottom. Scale bar: 300 μ m. Abbreviations: Gi, gigantocellular reticular nucleus; GiA, gigantocellular reticular nucleus, alpha part; IRt, intermediate reticular nucleus; PCrT, parvicellular reticular nucleus; ROb, raphe obscurus nucleus; RPa, pallidus; RMg, raphe magnus.

microinjection of the MC3/4-R agonist, MTII into the RPa area dose-dependently increases oxygen consumption in C57BL/6J mice, and inhibits food intake, whereas the antagonist SHU9119 enhances feeding in rats. These observations suggest that the RPa and adjacent area, in addition to containing the sympathetic premotor neurons and functioning as an important relay in the regulation of thermogenesis and thermoregulation^[23,27,29,38,41-43], also

contains a novel action site in the brainstem for the melanocortin system to coordinately regulate food intake and energy expenditure. This unique pathway of hypothalamic POMC neurons projecting to the RPa MC4-R-expressing neurons may play an important role in the central melanocortin system's regulation of energy balance by directly linking the integrated signals from hypothalamic POMC neurons to the downstream MC4-R neurons in the RPa

area of the brainstem, thereby altering their outputs and contributing to the balance of food intake and energy expenditure.

4.1 Innervation of RPa MC4-R neurons by α -MSH and the direct projection of hypothalamic POMC neurons to the RPa and adjacent area

Earlier studies have shown that α -MSH-IR and ACTH-IR fibers are present in the raphe nuclei and are moderately dense in the RMg in the rat^[44,45]. Consistent with and extending previous studies, our data shows that α -MSH-IR terminal fibers are in close apposition to MC4-R-GFP-expressing neurons in the RPa. This observation suggests that α -MSH, which is generally thought to be the endogenous agonist of melanocortin receptors, and post-translationally processed from its precursor POMC, is one of the neurotransmitter/modulators in the RPa area acting on MC4-R-bearing neurons to exert physiological functions. Indeed, our recent cellular electrophysiological data has demonstrated that α -MSH can excite a large subset of RPa neurons via a direct postsynaptic depolarization of the cells (Yan Gu *et al*, unpublished data).

Hypothalamic RCA/Arc neuronal projections to the RPa have been established by earlier CTB retrograde studies^[46], although the neurochemical identity of the hypothalamic neurons was not established. Similarly, an anterograde study showed that, upon Phaseolus vulgaris leucoagglutinin (PHA-L) iontophoresis into the Arc, PHA-L-IR fibers were identified in the RPa and RMg nuclei^[47]. Our data revealed that a high percentage (average 49%) of retrogradely-labeled neurons in the RCA/Arc co-expressed POMC-EGFP or POMC-IR (Figures 2 and 3 C, D, G, H). In contrast, almost no retrogradely-labeled POMC-EGFP or POMC-IR neurons were found in the cNTS of the brainstem, nor were retrogradely-labeled NPY-GFP-IR neurons found in the Arc. Consistent with the last result and in agreement with a previous study^[48], no AgRP-IR fibers were observed in the RPa and RMg area. Thus we have anatomically defined a unique melanocortin pathway from the hypothalamic POMC neurons directly projecting to the RPa MC4-R neurons.

4.2 Technical consideration

We employed a combination of retrograde tracing and ICC staining to identify the melanocortin innervations in the RPa area of mice and rats. The injection site was targeted to the rostral part of the RPa, the proposed sympathetic premotor nucleus regulating thermogenesis. However, the injected tracers inevitably spread into surrounding areas of the RPa. In most cases in mice, the injection site actually covered the RPa, RMg, part of the GiA and ventral

ROb. Therefore, in this study we refer to the injection site as the RPa and the adjacent area, which should include the RMg and parts of ROb and GiA. In fact, besides the RPa, neurons in immediately adjacent areas, including the RMg, part of GiA and the parapyramidal region also project to T3 of the IML^[49,50] and polysynaptically influence IBAT function^[28,38,51,52]. We estimated the extent of the subpopulation of RCA/Arc POMC neurons directly projecting to the RPa and adjacent area, rather than to the RPa itself.

4.3 Functional implications of MC4-R in the RPa area in the regulation of energy balance

The RPa and adjacent area has been proposed to contain the sympathetic premotor neurons controlling thermogenesis and thermoregulation^[25,28]. The RPa area is an important relay center mediating cold defense responses, including sympathetically-mediated IBAT non-shivering thermogenesis^[26,27,30,31,53], cutaneous vasoconstriction^[42,54] and the fusimotor activity^[43]. The RPa area is also essential in relaying central melanocortin-mediated thermogenesis^[23]. A large subset of MC4-R-GFP neurons in the RPa co-express pseudorabies virus (PRV)-IR after PRV injection into IBAT^[38] and α -MSH-IR terminal fibers innervate RPa neurons projecting to IBAT (our unpublished data). These data suggest that the brainstem RPa area contains a potential action site for the MC4-R-sympathetically-mediated regulation of BAT thermogenesis. Fourth ventricle injection of the MC3/4-R agonist MTII increased IBAT UCP1 mRNA expression in chronically decerebrate rats^[22], and 4th ventricle injection of MTII increases body temperature^[19] and oxygen consumption^[23]. Our data showing that microinjection of MTII into the RPa area dose-dependently increases oxygen consumption in C57BL/6J mice is consistent with and extends these previous studies. The data supports a hypothesis that the brainstem RPa area contains one of the action sites for brainstem MC4-R-mediated regulation of energy expenditure. BAT is a major thermogenic organ in rodents and it is estimated that thermogenesis in BAT may contribute to more than one-half of all oxygen consumption in a small animal in the cold^[55]. However, increased metabolism in other oxygen-consuming tissues besides BAT, for example, an alteration of cardiac activity, could have contributed to the oxygen consumption determination^[23]. Since excitation of RPa area neurons increased both IBAT thermogenesis and heart rate^[25,27], as did 4th ventricle injection of MTII^[19,22], the exact underlying mechanisms of increased oxygen consumption by activation of RPa MC4-Rs need to be further elucidated. It remains unclear if RPa MC4-R signals are required or sufficient for melanocortin-medi-

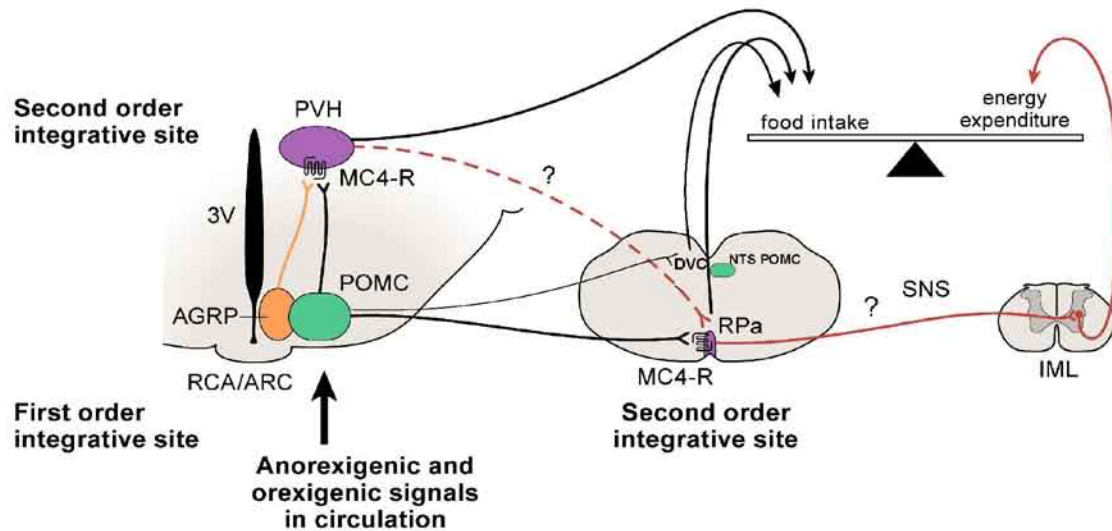


Figure 6. Model for the projection of hypothalamic POMC neurons to the RPa MC4-R neurons pathway in the regulation of energy balance by the central melanocortin circuitry. Schematic drawing illustrating that the medullary RPa and the adjacent area contain a second order integrative site in the central melanocortin circuitry regulating energy intake and expenditure. The central melanocortin circuits consist of multiple pathways at various levels of the brain to regulate energy balance. The unique intrinsic pathway from hypothalamic POMC neurons projecting to medullary RPa MC4-R neurons may play an important role in energy homeostasis by interacting with other melanocortin pathways. The MC4-R signaling in the RPa area regulates not only thermogenesis, but also food intake. The other potential pathways include hypothalamic POMC/AgRP to the PVH/DMH/LH MC4-R neuronal pathways, the hypothalamic POMC/AgRP to the DVC MC4-R neuronal pathway, and the hypothalamic POMC/CART to the IML MC4-R neuronal pathway. Acting together, these pathways may work to accomplish the coordinated regulation of energy balance.

ated diet-induced thermogenesis^[38,56].

Additionally, we have demonstrated that administration of MTII, or the MC3/4-R antagonist SHU9119 into the RPa area of rats dose-dependently inhibits or stimulates food intake, respectively. It has been reported that the neurons in the RPa project to the DVC^[57,58], and RPa stimulation causes a vagal dependent increase in gastric contractility via TRH projections to the DVC^[59,60]. However, it remains to be determined whether RPa MC4-R-regulated food intake is vagal dependent or not. Although the underlying mechanisms need further studying, our data suggest that the hypothalamic POMC-RPa MC4-R neuronal pathway may significantly contribute to the tonic inhibition of food intake exerted by the central melanocortin system^[1,5].

4.4 A working model for the central melanocortin system regulating energy balance

By extending our understanding of the melanocortin circuits regulating energy balance, the results outlined in this study have not only revealed a novel specific pathway of hypothalamic POMC neurons directly projecting to the RPa area, but also provided functional evidence that the RPa area may contain a novel action site in the brainstem for the melanocortin system coordinated regulation

of energy balance (Figure 6). The results favor a working model that the central melanocortin system recruits multiple neuronal pathways at various levels of the brain through their complex interactions to regulate energy intake and expenditure, thereby maintaining energy homeostasis when an animal confronts environmental nutrient challenges. These melanocortin pathways certainly include, but are not limited to, the hypothalamic POMC to RPa MC4-R neuronal pathway identified in this study, the proposed hypothalamic POMC/AgRP to PVH MC4-R pathway, the presumptive hypothalamic POMC/AgRP to DMH and LH pathways^[5,6,8,9], and the hypothalamic POMC to brainstem DVC MC4-R pathway^[19]. There has also been proposed a hypothalamic POMC/CART to IML of the spinal cord pathway, which could be activated by leptin and may contribute to increased thermogenesis and energy expenditure and decreased body weight following leptin administration^[61]. NTS POMC neurons can be activated by re-feeding^[17], by peripheral application of the short term satiety signal CCK^[17,18] and the long term adipostatic signal leptin^[62]. These data suggest that the brainstem NTS POMC neurons, like Arc POMC neurons, may also function as a first-order integrative site that can directly sense and integrate both the short term signals reflecting nutrient availability and the long term signals

reflecting energy storage. However, the secondary integrative sites downstream of the NTS POMC neurons remain to be clarified. Elucidating how these melanocortin pathways interact and how they contribute to the regulation of energy balance will be of great significance for a comprehensive understanding of the melanocortin circuits in energy homeostasis.

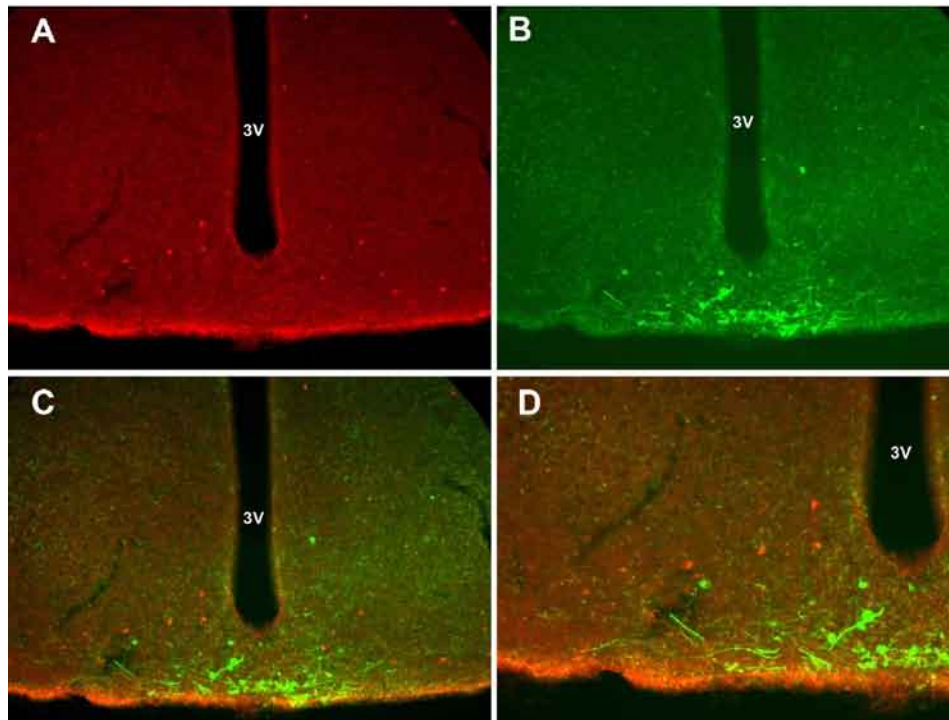
Acknowledgments

We would like to thank Dr. Jeffrey M. Friedman and Dr. Hongyan Liu for providing MC4-R-GFP and NPY-GFP transgenic mice, respectively, and Lori Vaskalis for assistance with illustrations.

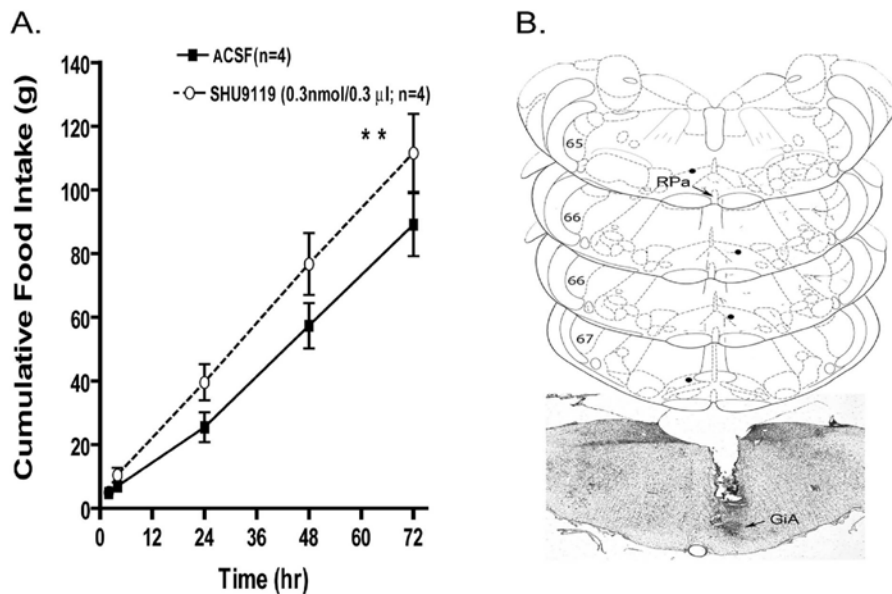
References

- Fan W, Boston BA, Kesterson RA, Hruby VJ, Cone RD. Role of melanocortinergic neurons in feeding and the agouti obesity syndrome. *Nature* 1997; 385: 165 – 8.
- Huszar D, Lynch CA, Fairchild-Huntress V, Dunmore JH, Fang Q, Berkemeier LR, Gu W, Kesterson RA, Boston BA, Cone RD, Smith FJ, Campfield LA, Burn P, Lee F. Targeted disruption of the melanocortin-4 receptor results in obesity in mice. *Cell* 1997; 88: 131 – 41.
- Yeo GS, Farooqi IS, Aminian S, Halsall DJ, Stanhope RG, O'Rahilly S. A frameshift mutation in MC4-R associated with dominantly inherited human obesity. *Nat Genet* 1998; 20: 111 – 2.
- Farooqi IS, Keogh JM, Yeo GS, Lank EJ, Cheetham T, O'Rahilly S. Clinical spectrum of obesity and mutations in the melanocortin 4 receptor gene. *N Engl J Med* 2003; 348: 1085 – 95.
- Cowley MA, Pronchuk N, Fan W, Dinulescu DM, Colmers WF, Cone RD. Integration of NPY, AGRP, and melanocortin signals in the hypothalamic paraventricular nucleus: evidence of a cellular basis for the adipostat. *Neuron* 1999; 24: 155 – 63.
- Barsh GS, Schwartz MW. Genetic approaches to studying energy balance: perception and integration. *Nat Rev Genet* 2002; 3: 589 – 600.
- Elmquist JK. Hypothalamic pathways underlying the endocrine, autonomic, and behavioral effects of leptin. *Physiol Behav* 2001; 74: 703 – 8.
- Badman MK, Flier JS. The gut and energy balance: visceral allies in the obesity wars. *Science* 2005; 307: 1909 – 14.
- Seeley RJ, Woods SC. Monitoring of stored and available fuel by the CNS: implications for obesity. *Nat Rev Neurosci* 2003; 4: 901 – 9.
- Cowley MA, Smart JL, Rubinstein M, Cerdan MG, Diano S, Horvath TL, Cone RD, Low MJ. Leptin activates anorexigenic POMC neurons through a neural network in the arcuate nucleus. *Nature* 2001; 411: 480 – 4.
- Cone RD, Cowley MA, Butler AA, Fan W, Marks DL, Low MJ. The arcuate nucleus as a conduit for diverse signals relevant to energy homeostasis. *Int J Obes Relat Metab Disord* 2001; 25(Suppl 5): S63 – 7.
- Elias CF, Aschkenasi C, Lee C, Kelly J, Ahima RS, Bjorbaek C, Flier JS, Saper CB, Elmquist JK. Leptin differentially regulates NPY and POMC neurons projecting to the lateral hypothalamic area. *Neuron* 1999; 23: 775 – 86.
- Schwartz MW, Seeley RJ, Woods SC, Weigle DS, Campfield LA, Burn P, Baskin DG. Leptin increases hypothalamic pro-opiomelanocortin mRNA expression in the rostral arcuate nucleus. *Diabetes* 1997; 46: 2119 – 23.
- Benoit SC, Air EL, Coolen LM, Strauss R, Jackman A, Clegg DJ, Seeley RJ, Woods SC. The catabolic action of insulin in the brain is mediated by melanocortins. *J Neurosci* 2002; 22: 9048 – 52.
- Cowley MA, Smith RG, Diano S, Tschop M, Pronchuk N, Grove KL, Strasburger CJ, Bidlingmaier M, Esterman M, Heiman ML, Garcia-Segura LM, Nillni EA, Mendez P, Low MJ, Sotonyi P, Friedman JM, Liu H, Pinto S, Colmers WF, Cone RD, Horvath TL. The distribution and mechanism of action of ghrelin in the CNS demonstrates a novel hypothalamic circuit regulating energy homeostasis. *Neuron* 2003; 37: 649 – 61.
- Balthasar N, Dalaard LT, Lee CE, Yu J, Funahashi H, Williams T, Ferreira M, Tang V, McGovern RA, Kenny CD, Christiansen LM, Edelstein E, Choi B, Boss O, Aschkenasi C, Zhang CY, Mountjoy K, Kishi T, Elmquist JK, Lowell BB. Divergence of melanocortin pathways in the control of food intake and energy expenditure. *Cell* 2005; 123: 493 – 505.
- Fan W, Ellacott KL, Halatchev IG, Takahashi K, Yu P, Cone RD. Cholecystokinin-mediated suppression of feeding involves the brainstem melanocortin system. *Nat Neurosci* 2004; 7: 335 – 6.
- Appleyard SM, Bailey TW, Doyle MW, Jin YH, Smart JL, Low MJ, Andresen MC. Proopiomelanocortin neurons in nucleus tractus solitarius are activated by visceral afferents: regulation by cholecystokinin and opioids. *J Neurosci* 2005; 25: 3578 – 85.
- Zheng H, Patterson LM, Phifer CB, Berthoud HR. Brain stem melanocortinergic modulation of meal size and identification of hypothalamic POMC projections. *Am J Physiol Regul Integr Comp Physiol* 2005; 289: R247 – 58.
- Grill HJ, Ginsberg AB, Seeley RJ, Kaplan JM. Brainstem application of melanocortin receptor ligands produces long-lasting effects on feeding and body weight. *J Neurosci* 1998; 18: 10128 – 35.
- Williams DL, Kaplan JM, Grill HJ. The role of the dorsal vagal complex and the vagus nerve in feeding effects of melanocortin-3/4 receptor stimulation. *Endocrinology* 2000; 141: 1332 – 7.
- Williams DL, Bowers RR, Bartness TJ, Kaplan JM, Grill HJ. Brainstem melanocortin 3/4 receptor stimulation increases uncoupling protein gene expression in brown fat. *Endocrinology* 2003; 144: 4692 – 7.
- Fan W, Morrison SF, Cao WH, Yu P. Thermogenesis activated by central melanocortin signaling is dependent on neurons in the rostral raphe pallidus (rPa) area. *Brain Res* 2007; 1179: 61 – 9.
- Bachman ES, Dhillon H, Zhang CY, Cinti S, Bianco AC, Kobilka BK, Lowell BB. Beta AR signaling required for diet-induced thermogenesis and obesity resistance. *Science* 2002; 297: 843 – 5.
- Morrison SF, Sved AF, Passerin AM. GABA-mediated inhibition of raphe pallidus neurons regulates sympathetic outflow to brown adipose tissue. *Am J Physiol* 1999; 276: R290 – 7.
- Nakamura K, Matsumura K, Kaneko T, Kobayashi S, Katoh H, Negishi M. The rostral raphe pallidus nucleus mediates pyrogenic transmission from the preoptic area. *J Neurosci* 2002; 22: 4600 – 10.
- Zaretsky DV, Zaretskaia MV, DiMicco JA. Stimulation and blockade of GABA(A) receptors in the raphe pallidus: effects on body temperature, heart rate, and blood pressure in conscious rats. *Am J Physiol Regul Integr Comp Physiol* 2003; 285: R110 – 6.
- Nakamura K, Matsumura K, Hubschle T, Nakamura Y, Hioki H, Fujiyama F, Boldogkoi Z, Konig M, Thiel HJ, Gerstberger R, Kobayashi S, Kaneko T. Identification of sympathetic premotor neurons in medullary raphe regions mediating fever and other thermoregulatory functions. *J Neurosci* 2004; 24: 5370 – 80.
- Morrison SF. Differential control of sympathetic outflow. *Am J Physiol Regul Integr Comp Physiol* 2001; 281: R683 – 98.
- Cao WH, Fan W, Morrison SF. Medullary pathways mediating specific sympathetic responses to activation of dorsomedial hypothalamus. *Neuroscience* 2004; 126: 229 – 40.
- Morrison SF. Activation of 5-HT1A receptors in raphe pallidus inhibits leptin-evoked increases in brown adipose tissue thermogenesis. *Am J Physiol Regul Integr Comp Physiol* 2004; 286: R832 – 7.
- Mountjoy KG, Mortrud MT, Low MJ, Simerly RB, Cone RD. Localization of the melanocortin-4 receptor (MC4-R) in neuroendocrine and autonomic control circuits in the brain. *Mol Endocrinol* 1994; 8: 1298 – 308.
- Kishi T, Aschkenasi CJ, Lee CE, Mountjoy KG, Saper CB, Elmquist

- JK. Expression of melanocortin 4 receptor mRNA in the central nervous system of the rat. *J Comp Neurol* 2003; 457: 213 – 35.
34. Liu H, Kishi T, Roseberry AG, Cai X, Lee CE, Montez JM, Friedman JM, Elmquist JK. Transgenic mice expressing green fluorescent protein under the control of the melanocortin-4 receptor promoter. *J Neurosci* 2003; 23: 7143 – 54.
35. Heisler LK, Jobst EE, Sutton GM, Zhou L, Borok E, Thornton-Jones Z, Liu HY, Zigman JM, Balthasar N, Kishi T, Lee CE, Aschkenasi CJ, Zhang CY, Yu J, Boss O, Mountjoy KG, Clifton PG, Lowell BB, Friedman JM, Horvath T, Butler AA, Elmquist JK, Cowley MA. Serotonin reciprocally regulates melanocortin neurons to modulate food intake. *Neuron* 2006; 51: 239 – 49.
36. Hahn TM, Breininger JF, Baskin DG, Schwartz MW. Coexpression of *Agrp* and *NPY* in fasting-activated hypothalamic neurons. *Nat Neurosci* 1998; 1: 271 – 2.
37. Chen P, Li C, Haskell-Luevano C, Cone RD, Smith MS. Altered expression of agouti-related protein and its colocalization with neuropeptide Y in the arcuate nucleus of the hypothalamus during lactation. *Endocrinology* 1999; 140: 2645 – 50.
38. Voss-Andreae A, Murphy JG, Ellacott KL, Stuart RC, Nillni EA, Cone RD, Fan W. Role of the central melanocortin circuitry in adaptive thermogenesis of brown adipose tissue. *Endocrinology* 2007; 148: 1550 – 60.
39. Cone RD. The central melanocortin system and energy homeostasis. *Trends Endocrinol Metab* 1999; 10: 211 – 6.
40. Cone RD. Anatomy and regulation of the central melanocortin system. *Nat Neurosci* 2005; 8: 571 – 8.
41. Fan W, Voss-Andreae A, Cao WH, Morrison SF. Regulation of thermogenesis by the central melanocortin system. *Peptides* 2005; 26: 1800 – 13.
42. Blessing WW. Lower brainstem pathways regulating sympathetically mediated changes in cutaneous blood flow. *Cell Mol Neurobiol* 2003; 23: 527 – 38.
43. Tanaka M, Owens NC, Nagashima K, Kanosue K, McAllen RM. Reflex activation of rat fusimotor neurons by body surface cooling, and its dependence on the medullary raphe. *J Physiol* 2006; 572: 569 – 83.
44. Romagnano MA, Joseph SA. Immunocytochemical localization of ACTH1-39 in the brainstem of the rat. *Brain Res* 1983; 276: 1 – 16.
45. Yamazoe M, Shiosaka S, Yagura A, Kawai Y, Shibasaki T, Ling N, Tohyama M. The distribution of alpha-melanocyte stimulating hormone (alpha-MSH) in the central nervous system of the rat: an immunohistochemical study. II. Lower brain stem. *Peptides* 1984; 5: 721 – 7.
46. Hermann DM, Luppi PH, Peyron C, Hinckel P, Jouvet M. Afferent projections to the rat nuclei raphe magnus, raphe pallidus and reticularis gigantocellularis pars alpha demonstrated by iontophoretic application of cholera toxin (subunit b). *J Chem Neuroanat* 1997; 13: 1 – 21.
47. Sim LJ, Joseph SA. Arcuate nucleus projections to brainstem regions which modulate nociception. *J Chem Neuroanat* 1991; 4: 97 – 109.
48. Bagnol D, Lu XY, Kaelin CB, Day HE, Ollmann M, Gantz I, Akil H, Barsh GS, Watson SJ. Anatomy of an endogenous antagonist: relationship between Agouti-related protein and proopiomelanocortin in brain. *J Neurosci* 1999; 19(RC26): 1 – 7.
49. Sasek CA, Helke CJ. Enkephalin-immunoreactive neuronal projections from the medulla oblongata to the intermediolateral cell column: relationship to substance P-immunoreactive neurons. *J Comp Neurol* 1989; 287: 484 – 94.
50. Sasek CA, Wessendorf MW, Helke CJ. Evidence for co-existence of thyrotropin-releasing hormone, substance P and serotonin in ventral medullary neurons that project to the intermediolateral cell column in the rat. *Neuroscience* 1990; 35: 105 – 19.
51. Bamshad M, Song CK, Bartness TJ. CNS origins of the sympathetic nervous system outflow to brown adipose tissue. *Am J Physiol* 1999; 276: R1569 – 78.
52. Cano G, Passerin AM, Schiltz JC, Card JP, Morrison SF, Sved AF. Anatomical substrates for the central control of sympathetic outflow to interscapular adipose tissue during cold exposure. *J Comp Neurol* 2003; 460: 303 – 26.
53. Morrison SF. Raphe pallidus neurons mediate prostaglandin E2-evoked increases in brown adipose tissue thermogenesis. *Neuroscience* 2003; 121: 17 – 24.
54. Tanaka M, Nagashima K, McAllen RM, Kanosue K. Role of the medullary raphe in thermoregulatory vasomotor control in rats. *J Physiol* 2002; 540: 657 – 64.
55. Cannon B, Nedergaard J. Brown adipose tissue: function and physiological significance. *Physiol Rev* 2004; 84: 277 – 359.
56. Butler AA, Marks DL, Fan W, Kuhn CM, Bartolome M, Cone RD. Melanocortin-4 receptor is required for acute homeostatic responses to increased dietary fat. *Nat Neurosci* 2001; 4: 605 – 11.
57. Palkovits M, Mezey E, Eskay RL, Brownstein MJ. Innervation of the nucleus of the solitary tract and the dorsal vagal nucleus by thyrotropin-releasing hormone-containing raphe neurons. *Brain Res* 1986; 373: 246 – 51.
58. Lynn RB, Kreider MS, Miselis RR. Thyrotropin-releasing hormone-immunoreactive projections to the dorsal motor nucleus and the nucleus of the solitary tract of the rat. *J Comp Neurol* 1991; 311: 271 – 88.
59. Garrick T, Yang H, Trauner M, Livingston E, Tache Y. Thyrotropin-releasing hormone analog injected into the raphe pallidus and obscurus increases gastric contractility in rats. *Eur J Pharmacol* 1992; 223: 75 – 81.
60. Garrick T, Prince M, Yang H, Ohning G, Tache Y. Raphe pallidus stimulation increases gastric contractility via TRH projections to the dorsal vagal complex in rats. *Brain Res* 1994; 636: 343 – 7.
61. Elias CF, Lee C, Kelly J, Aschkenasi C, Ahima RS, Couceyro PR, Kuhar MJ, Saper CB, Elmquist JK. Leptin activates hypothalamic CART neurons projecting to the spinal cord. *Neuron* 1998; 21: 1375 – 85.
62. Ellacott KL, Halatchev IG, Cone RD. Characterization of leptin-responsive neurons in the caudal brainstem. *Endocrinology* 2006; 147: 3190 – 5.



Supplementary Figure 1. Photomicrograph showing the distribution of CTB-IR and NPY-GFP-IR neurons in the Arc of the hypothalamus following CTB injection into the RPa in NPY-GFP transgenic mice. (A – C): Distribution of CTB-IR (red, A), NPY-GFP-IR (green, B) and merged image of A and B, C. (D): Higher magnification of C. Note no double labeling of CTB-IR and NPY-GFP-IR neurons could be found. Scale bar: 100 μ m.



Supplementary Figure 2. Effects of the MC3/4-R antagonist SHU9119 injected into one side of GiA on food intake. (A) Microinjection of MC3/4-R antagonist SHU9119 (0.3 nmol, 0.3 μ l) into the GiA significantly stimulated food intake in rats ($P < 0.01$, $n = 4$). (B). The placement of microinjection sites aimed at the GiA of rats are shown on modified atlas drawings approximately from 11.3 to 11.8 mm caudal to bregma, with the atlas figure numbers on the left side of each section (Paxinos, 1998). Filled circles indicate the locations of dye spots marking the injection sites in the GiA region of the ventromedial medulla in 4 rats. A photomicrograph of a representative histological coronal section containing a microinjection site in the GiA region of the ventromedial medulla of a rat is shown on the bottom.